

# SCIENTIFIC REPORTS



OPEN

## Hot electron induced non-saturation current behavior at high electric field in InAlN/GaN heterostructures with ultrathin barrier

Lei Guo<sup>1</sup>, Xuelin Yang<sup>1</sup>, Anqi Hu<sup>1</sup>, Zhihong Feng<sup>2</sup>, Yuanjie Lv<sup>2</sup>, Jie Zhang<sup>1</sup>, Jianpeng Cheng<sup>1</sup>, Ning Tang<sup>1</sup>, Xinqiang Wang<sup>1,3</sup>, Weikun Ge<sup>1</sup> & Bo Shen<sup>1,3</sup>

The high-field transport characteristics of nearly lattice-matched InAlN/GaN heterostructures with different barrier thickness were investigated. It is found that the current in the InAlN/GaN heterostructures with ultrathin barrier shows unsaturated behaviors (or secondary rising) at high voltage, which is different from that of AlGaIn/GaN heterostructures. This phenomenon is more obvious if the barrier thickness is thinner and the channel width is narrower. The experimental results demonstrate that it is the increasing carrier density excited from the more defect states by the hot electrons with larger electron saturation velocity that results in the unsaturated current behaviors in InAlN/GaN heterostructures. Our results pave a way for further optimizing InAlN barrier design and improving the reliability of InAlN/GaN HEMTs.

GaN-based high electron mobility transistors (HEMTs) are promising devices for next generation high frequency and high power applications<sup>1–2</sup>. In particular, InAlN/GaN HEMTs are excellent alternatives to AlGaIn/GaN HEMTs for ultrahigh frequency device applications. The current gain cutoff frequency of ultrascaled InAlN/GaN HEMTs has already been up to 400 GHz, as reported recently<sup>3–5</sup>. However, several questions related to the device reliability at high electric field are still open for InAlN/GaN HEMTs. On one hand, compared to AlGaIn, the material quality of InAlN still need to be improved due to the different optimized growth conditions of In and AlN and the expected large immiscibility gap of the ternary alloy. Thus, there are large density of defects which may correlate to the problem of more serious degradation of the InAlN/GaN HEMTs<sup>6–8</sup>. On the other hand, the larger spontaneous polarization in InAlN/GaN heterostructures contributes to much higher two-dimensional electron gas (2DEG) density in the lattice-matched In<sub>0.18</sub>Al<sub>0.82</sub>N/GaN system with thin barrier layer<sup>9,10</sup>. Some studies have proved that the higher electron density of InAlN/GaN may result in lower hot phonon (HP) lifetime and weaker HP effect, and thus lead to higher electron velocity and larger kinetic energy than that of AlGaIn/GaN heterostructure<sup>11–14</sup>. Although the higher electron velocity is benefit to high frequency devices, the hot-electron temperature ( $T_e$ ) in InAlN/GaN is much higher than that in AlGaIn/GaN. For example, Kuzmik *et al.* reported that  $T_e$  in InAlN/GaN may reach as high as 30000 K<sup>6,15</sup>. Considering the hot electrons with higher energy and facing larger defects density, the transport characteristics of InAlN/GaN at high electric field are more complex and lack of systematic studies, compared with that of AlGaIn/GaN. Especially, the behavior of the current at high field in InAlN/GaN is quite different from that in AlGaIn/GaN, the saturation tendency of the current observed in the latter cannot be observed again in InAlN/GaN heterostructures<sup>16</sup>. Detailed mechanism about this phenomenon is yet to be fully understood, although it is important for further improving the reliability of InAlN/GaN HEMTs. In this work, we investigate the high-field transport characteristics of In<sub>0.18</sub>Al<sub>0.82</sub>N/GaN with different

<sup>1</sup>State Key Laboratory of Artificial Microstructure and Mesoscopic Physics, School of Physics, Peking University, Beijing 100871, China. <sup>2</sup>National Key Laboratory of Application Specific Integrated Circuit, Hebei Semiconductor Research Institute, Shijiazhuang 050051, China. <sup>3</sup>Collaborative Innovation Center of Quantum Matter, Beijing 100871, China. Correspondence and requests for materials should be addressed to X.Y. (email: xlyang@pku.edu.cn) or B.S. (email: bshen@pku.edu.cn)

Samples	Barrier layer	Barrier thickness (nm)	Density ( $\times 10^{12} \text{ cm}^{-2}$ )	Mobility ( $\text{cm}^2/\text{Vs}$ )
# 1	$\text{In}_{0.18}\text{Al}_{0.82}\text{N}$	4	17.5	1500
# 2	$\text{In}_{0.18}\text{Al}_{0.82}\text{N}$	8	23.5	1400
# 3	$\text{In}_{0.18}\text{Al}_{0.82}\text{N}$	100	26.0	790
# 4	$\text{Al}_{0.24}\text{Ga}_{0.76}\text{N}$	20	8.1	2050

**Table 1.** Sample structures and electrical properties measured at room temperature.

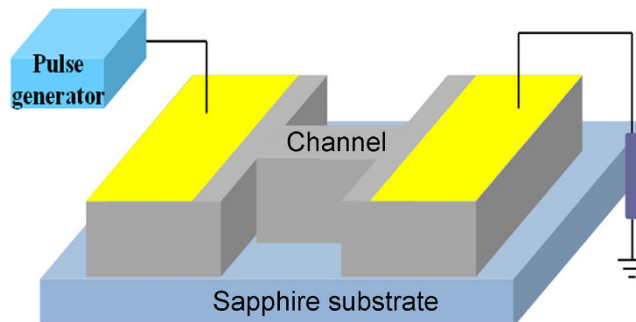


**Figure 1.** The schematic H-shaped test structure used for the measurements.

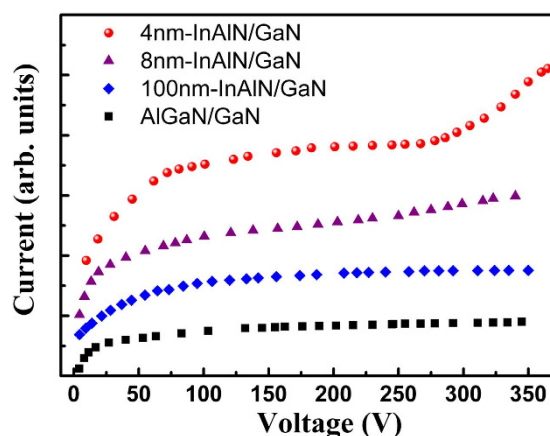


**Figure 2.** I-V characteristics of the AlGaN/GaN and InAlN/GaN heterostructures with different barrier thickness.

InAlN barrier thickness. Different from that of AlGaN/GaN, the current in the InAlN/GaN heterostructure with ultrathin barrier shows obvious secondary rising after a saturation region at higher voltage. It is demonstrated that the phenomenon is related with the larger electron kinetic energy as well as the larger density of defects. In fact, it is the increased carrier density excited from the defect states by hotter electrons leads to the secondary rising current in the InAlN/GaN heterostructure.

Table 1 shows the sample information including barrier thickness, electron mobility ( $\mu$ ) and sheet density ( $n$ ) measured at room temperature by a Hall Effect measurement system with Van der Pauw method. With the thickness of the InAlN barrier increasing from 4 to 100 nm, the electron sheet density increases from  $1.75 \times 10^{13}$  to  $2.60 \times 10^{13} \text{ cm}^{-2}$ , and the mobility decreases from 1500 to  $790 \text{ cm}^2/\text{Vs}$ . Figure 1 gives the schematic H-shaped test structure. The current-voltage (I-V) curves of the AlGaN/GaN heterostructure shown in the Fig. 2 are the typical characteristics for GaN-based material system<sup>17</sup>. When the applied voltage changing from low to high values, there appear three regions that show different relationships between current and voltage. At the low electric field region, there is a linear relation where the Ohm's law is obeyed, and the current linearly relies on the voltage. With further increasing voltage, the relation becomes sublinear, which is due to the fact that the electron energy is gradually enhanced and so that more serious scattering is induced, leading to electron mobility decrease and a sublinear dependence between current and voltage. Finally, when the voltage is above 80 V (about 80 kV/cm for the electric field), the current gradually rises into the saturation region, the saturation velocity ( $v_{sat}$ ) can be inferred from current density:

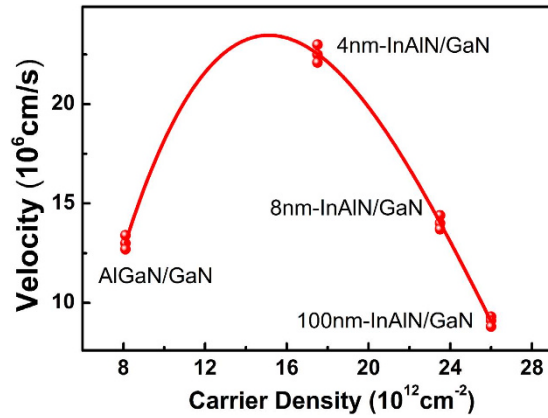


**Figure 3.** Dependence of experimental saturation velocity on carrier density for different samples shown in Table 1. The channel dimensions ( $L \times W$ ) of testing samples is  $10 \mu\text{m} \times 15 \mu\text{m}$ . The scattered data represent results of different areas from the same wafer.

$$J = env, \quad (1)$$

where  $e$  is the charge of electron,  $n$  is the sheet density, and  $v$  is the electron drift mobility. According to equation (1), the saturation velocity is calculated to be about  $1.3 \times 10^7 \text{ cm/s}$ , as shown in Fig. 3. It should be mentioned that the saturation velocity  $v_{sat}$  is theoretically determined by the longitudinal optical (LO) phonon and should be of the order of:

$$v_{sat} = \sqrt{\hbar\omega_{LO}/m_e} \approx 3 \times 10^7 \text{ cm/s}, \quad (2)$$

where  $\hbar\omega_{LO}$  is the energy of the LO phonon, and  $m_e$  is the electron effective mass. However, the measured  $v_{sat}$  in GaN is much lower than the theoretical value, which is mainly caused by the HP effect due to the large number of hot phonons. It is noticed that the LO phonon lifetime ( $\sim 0.35\text{--}2.5 \text{ ps}$ ) is much longer than the spontaneous LO phonon emission time ( $\sim 10 \text{ fs}$ ), so that there will be a great accumulation of phonons in the system. The accumulated none-equilibrium LO phonons emitted by hot electrons can reduce the energy relaxation rate and enhance the momentum relaxation rate of the hot electrons. Thus,  $v_{sat}$  is much lower due to more serious momentum scattering<sup>18,19</sup>. In brief, the lower  $v_{sat}$  is mainly limited by the longer hot phonon lifetime.

As shown in Fig. 2, the I-V characteristics of a 100 nm-thick barrier InAlN/GaN is similar with that of AlGaIn/GaN heterostructure, and the current gradually increases to saturation with increasing voltage. However, as the InAlN barrier thickness decreases to 8 nm, it is interesting to find that the current shows a secondary slightly rising behavior after saturation with further increasing voltage. The phenomenon of the secondary rising at sufficiently high voltage is more obvious when the InAlN barrier thickness further decreases to 4 nm. For 4 nm-thick barrier InAlN/GaN, with voltage increasing from 6 V to 80 V, the I-V characteristic changes from linear to sub-linear. Further increasing the voltage from 80 V to 260 V, the current basically keeps the saturation value due to the velocity saturation. The  $v_{sat}$  inferred from the saturation current in the InAlN/GaN heterostructure with 4 nm-thick-InAlN barrier is about  $2.3 \times 10^7 \text{ cm/s}$  (shown in Fig. 3) which is much higher than that in AlGaIn/GaN heterostructures. However when the voltage is above a critical voltage, the current shows a surprising secondary rising with the voltage increasing from 270 V to 360 V, and no saturation tendency is observed. It should be mentioned that the current density rising could be due to the increasing of either carrier sheet density or velocity, according to equation (1). At the low voltage region (linear and sublinear region), the rising of current is due to the increased velocity. But that is not the cause for the secondary rising at the high voltage range, since the saturation velocity is determined by the energy of the LO phonon as mentioned above, being independent on the voltage. In addition, if the carrier density is constant and independent on the voltage, the inferred velocity at 360 V would be up to about  $3.3 \times 10^7 \text{ cm/s}$  which is much higher over the theoretical upper limit value, hence not possible. Therefore, the secondary rising of the current should mainly result from the increased carrier density induced by the interaction between the hot electrons and material defects.

To further understand the above phenomenon, there are two questions need to be addressed at first: (i) why does the secondary rising happen in InAlN/GaN but not in AlGaIn/GaN heterostructures, despite that they have the same GaN channel; (ii) why is the phenomenon more obvious in the sample with 4 nm barrier than that with thicker barrier? We can find answers from the view point of hot electron behaviors and material defects.

Firstly, the value of  $v_{sat}$  for the hot electron as a function of the carrier density was extracted (Fig. 3) according to equation (1) for different samples. With the electron density increasing from  $8.0 \times 10^{12} \text{ cm}^{-2}$  in AlGaIn/GaN heterostructure to  $17.5 \times 10^{12} \text{ cm}^{-2}$  in the InAlN/GaN heterostructure with 4 nm-InAlN barrier, the value of  $v_{sat}$  increases from  $1.3 \times 10^7 \text{ cm/s}$  to  $2.3 \times 10^7 \text{ cm/s}$ , reaching a highest value. Then, with the electron density further increasing to  $23.5 \times 10^{12} \text{ cm}^{-2}$  in the 8 nm-InAlN barrier sample and finally increasing to  $26.0 \times 10^{12} \text{ cm}^{-2}$  in the 100-nm InAlN barrier sample,  $v_{sat}$  gradually decreases down to  $0.9 \times 10^7 \text{ cm/s}$ . As discussed above,  $v_{sat}$  is mainly related with the HP lifetime, the variation pattern of  $v_{sat}$  is consistent with that of the HP lifetime as previous

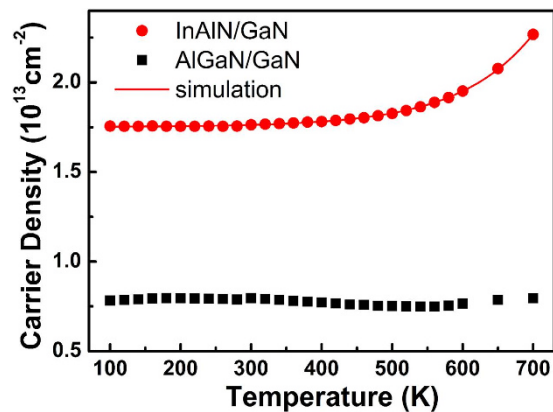


**Figure 4.** Temperature-dependence carrier density of the AlGaIn/GaN heterostructure and InAlN/GaN heterostructure with 4 nm-InAlN barrier.

reported: the HP lifetime is closely related to the electron density due to plasma-LO phonon coupling, the estimated resonant density is about  $7.0 \times 10^{12} \text{ cm}^{-2}$  and shifts to higher values with increasing the applied power<sup>13,20</sup>. When the electron density is below that value, the HP lifetime will decrease with increasing density and thus  $v_{sat}$  will increase, which is consistent with the results in the present work referring to the sample change from AlGaIn/GaN heterostructure to InAlN/GaN heterostructure with 4 nm-barrier. The case is converse when the density is beyond that value: the HP lifetime will increase with increasing density and thus  $v_{sat}$  will decrease, that can perfectly explain the results of InAlN/GaN with different barrier thickness.

The temperature-dependence of the 2DEG sheet density of the InAlN/GaN heterostructure (4 nm-barrier) and AlGaIn/GaN heterostructure are shown in Fig. 4. In the temperature range of 100–700 K, the carrier density of AlGaIn/GaN has a weak dependence on temperature, showing a typical 2DEG behavior. However, the temperature-dependence of the density in the InAlN/GaN heterostructure shows a standard shallow-donor behavior. The activation energy of the donor is around 90 meV from the fitting result using a donor model. Since the GaN buffer is the same between the AlGaIn/GaN and InAlN/GaN heterostructure, the donor may exist in the InAlN layer or interface. It should be mentioned that there are also other defect states with deeper level existing in the InAlN layer or interface, as revealed by capacitance-voltage and deep-level transient spectroscopy experiments<sup>8,21–23</sup>. The donor defect with an activation energy of 90 meV exhibited by the temperature-dependence Hall measurement is just the most easily excited by the high temperature and contributes to the sheet density. In fact, the hot electron temperature in the InAlN/GaN heterostructure may be much higher than the upper limitation of the temperature range in our Hall testing system. Therefore, it is reasonable to deduce that the hot electrons can also easily excite the electrons trapped in the deeper defects states in the InAlN/GaN heterostructure, which may also contributes to the secondary rising behaviors.

Now, considering interaction between the hot electrons and material defects, it is easier to understand that the electrons trapped in these donor states are excited to conduction band by hot electron at high voltage and result in the secondary rising current in InAlN/GaN rather than AlGaIn/GaN. Moreover, higher  $v_{sat}$  in InAlN/GaN with lower carrier density corresponds to much larger kinetic energy which can more easily excite trapped electron into conduction band. Thus, the secondary rising current phenomenon is more obvious in the InAlN/GaN with 4 nm-barrier than that with thicker ones.

To further confirm our explanation, we prepared several test devices of the H-shaped geometry with different channel widths changing from 5 to 20  $\mu\text{m}$  for InAlN/GaN heterostructures with 4 nm-barrier. Our previous work has confirmed that narrower channel can enhance the momentum relaxation of LO phonons and lower the lifetime of HP, and thus help to increase  $v_{sat}$ <sup>24</sup>. According to this result, the hot electrons in a narrower channel have larger kinetic energy than that in a wider channel, and thus more easily excite the electrons trapped in defect states. Figure 5 shows the I-V characteristics of the devices with different channel widths. We can see that the current of the test device with 5  $\mu\text{m}$  width channel shows a larger secondary rising at a smaller voltage than that of devices with 15 and 20  $\mu\text{m}$  width channels. This result further confirms that the interaction between the hot electrons with large kinetic energy and the large density of defects are the main reason of the secondary rising current.

In summary, we have investigated the high-field transport properties of InAlN/GaN heterostructures. Different from that of AlGaIn/GaN, the current of InAlN/GaN heterostructure shows a secondary rising at higher voltage after a saturation region. The secondary rising phenomenon is more obvious in samples with thinner barrier thickness and narrower channel width. These behaviors are attributed to the larger electron kinetic energy and more defects in InAlN/GaN than that in AlGaIn/GaN heterostructures. It is the increasing carrier density excited from the defect states by hot electrons that results in the secondary rising current in InAlN/GaN heterostructures with ultrathin barrier. The present work highlights the importance of InAlN barrier thickness as well as the quality for improving the reliability of InAlN/GaN HEMTs.

## Methods

**Sample Preparation.** The  $\text{In}_{0.18}\text{Al}_{0.82}\text{N}/\text{GaN}$  and  $\text{Al}_{0.24}\text{Ga}_{0.76}\text{N}/\text{GaN}$  heterostructures used in this work were grown on *c*-plane sapphire substrate by metal-organic chemical vapor deposition (MOCVD). The

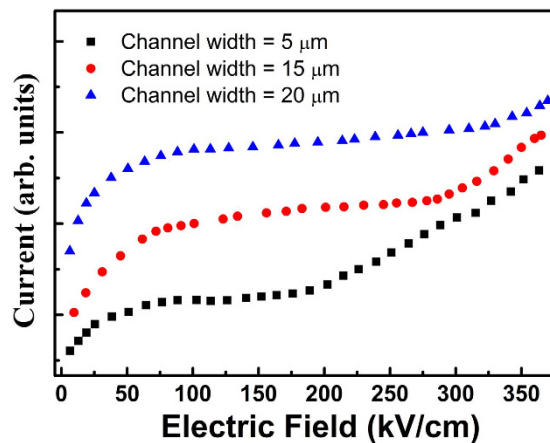


**Figure 5.** Dependence of current on electric field for the InAlN/GaN heterostructure with 4 nm-barrier. Different curves represent the characteristics for the test devices with different channel widths changing from 5 to 20  $\mu\text{m}$ .

heterostructures consisted of a 2.5  $\mu\text{m}$  thick GaN buffer layer, a thin AlN spacer, and  $\text{In}_{0.18}\text{Al}_{0.82}\text{N}$  or  $\text{Al}_{0.24}\text{Ga}_{0.76}\text{N}$  barrier. The growth temperature for  $\text{In}_{0.18}\text{Al}_{0.82}\text{N}$  and  $\text{Al}_{0.24}\text{Ga}_{0.76}\text{N}$  is about 800 °C and 1070 °C, respectively. The channel dimensions ( $L \times W$ ) are 10  $\mu\text{m} \times 15 \mu\text{m}$ , and the mesa was etched down to the substrate. The sample's mesa was fabricated with an H-shaped geometry (Fig. 1) which may (i) make the electric field in the channel homogenous, (ii) minimize the effects of contact resistance, and (iii) control the carrier injection from the Ohmic contacts<sup>25</sup>. The Ohmic contacts (300  $\mu\text{m} \times 500 \mu\text{m}$ ) on both sides were processed by Ti/Al/Ni/Au metallization and annealed at 850 °C for 35 s. The contact resistance was 0.9  $\Omega \cdot \text{mm}$  estimated at low electric fields by transmission line model (TLM). The channel at the middle was passivated with a 100 nm  $\text{Si}_3\text{N}_4$  passivation layer.

**Measurements.** High-field current-voltage (I-V) characteristics were obtained by nanosecond pulsed technique on H-shape sample mounted in a 50  $\Omega$  matched circuit. The voltage pulse length was fixed at 80 ns with a repetition rate of 1 Hz in order to minimize the self-heating effect.

## References

- Chen, Z. *et al.* Growth of AlGaIn/GaN heterojunction field effect transistors on semi-insulating GaN using an AlGaIn interlayer. *Appl. Phys. Lett.* **94**, 112108 (2009).
- Lee, D. S., Liu, Z. & Palacios, T. GaN high electron mobility transistors for sub-millimeter wave applications. *Jpn. J. Appl. Phys.* **53**, 100212 (2014).
- Lee, D. S. *et al.* 300-GHz InAlN/GaN HEMTs With InGaIn Back Barrier. *IEEE Electron Device Lett.* **32**, 1525(2011).
- Yue, Y. *et al.* InAlN/AlN/GaN HEMTs With Regrown Ohmic Contacts and  $f_T$  of 370 GHz. *IEEE Electron Device Lett.* **33**, 988 (2012).
- Yue, Y. *et al.* Ultrascaled InAlN/GaN High Electron Mobility Transistors with Cutoff Frequency of 400 GHz. *Jpn. J. Appl. Phys.* **52**, 08JN14 (2013).
- Kuzmik, J. *et al.* Buffer-Related Degradation Aspects of Single and Double-Heterostructure Quantum Well InAlN/GaN High-Electron-Mobility Transistors. *Jpn. J. Appl. Phys.* **51**, 054102 (2012).
- Zhu, C. Y. *et al.* Degradation and phase noise of InAlN/AlN/GaN heterojunction field effect transistors: Implications for hot electron/phonon effects. *Appl. Phys. Lett.* **101**, 103502 (2012).
- Horcajo, S. M. *et al.* Trapping phenomena in AlGaIn and InAlN barrier HEMTs with different geometries. *Semicond. Sci. Technol.* **30**, 035015 (2015).
- Kuzmik, J. Power electronics on InAlN/(In)GaIn: Prospect for a record performance. *IEEE Electron Device Lett.* **22**, 510 (2001).
- Tulek, R. *et al.* Comparison of the transport properties of high quality AlGaIn/AlN/GaN and AlInN/AlN/GaN two-dimensional electron gas heterostructures. *J. Appl. Phys.* **105**, 013707 (2009).
- Ardaravičius, L. *et al.* Threshold field for soft damage and electron drift velocity in InGaIn two-dimensional channels. *Semicond. Sci. Technol.* **30**, 105016 (2015).
- Bajaj, S. *et al.* Density-dependent electron transport and precise modeling of GaN high electron mobility transistors. *Appl. Phys. Lett.* **107**, 153504 (2015).
- Leach, J. H. *et al.* Effect of hot phonon lifetime on electron velocity in InAlN/AlN/GaN heterostructure field effect transistors on bulk GaN substrates. *Appl. Phys. Lett.* **96**, 133505 (2010).
- Zhang, J. Z., Dyson, A. & Ridley, B. K. Hot electron energy relaxation in lattice-matched InAlN/AlN/GaN heterostructures: The sum rules for electron-phonon interactions and hot-phonon effect. *J. Appl. Phys.* **117**, 025701 (2015).
- Tapajna, M. *et al.* Hot electron related degradation in InAlN/GaN high electron mobility transistors. *IEEE Trans. Electron Devices* **61**, 2793 (2014).
- Ardaravičius, L. *et al.* Electron drift velocity in lattice-matched AlInN/AlN/GaN channel at high electric fields. *J. Appl. Phys.* **106**, 073708 (2009).
- Danilchenko, B. A. *et al.* Hot-electron transport in AlGaIn/GaN two-dimensional conducting channels. *Appl. Phys. Lett.* **85**, 5421 (2004).
- Matulionis, A. Hot phonons in GaN channels for HEMTs. *Phys. Status Solid. A* **203**, 2313 (2006).
- Guo, L. *et al.* Effects of light illumination on electron velocity of AlGaIn/GaN heterostructures under high electric field. *Appl. Phys. Lett.* **105**, 242104 (2014).
- Matulionis, A. *et al.* Plasmon-enhanced heat dissipation in GaN-based two-dimensional channels. *Appl. Phys. Lett.* **95**, 192102 (2009).
- Chen, Z. *et al.* Deep traps in InAlN lattice-matched to GaN grown by metal organic chemical vapor deposition studied by deep-level transient spectroscopy. *Jpn. J. Appl. Phys.* **50**, 081001 (2011).

22. Zhou, Y. *et al.* Analysis of interface trap states in InAlN/AlN/GaN heterostructures. *Semicond. Sci. Technol.* **29**, 095011 (2014).
23. Py, M. A. *et al.* Capacitance behavior of InAlN Schottky diodes in presence of large concentrations of shallow and deep states related to oxygen. *J. Appl. Phys.* **117**, 185701 (2015).
24. Ma, N. *et al.* Boundary-enhanced momentum relaxation of longitudinal optical phonons in GaN. *Appl. Phys. Lett.* **100**, 052109 (2012).
25. Ma, N. *et al.* Current-controlled negative differential resistance effect induced by Gunn-type instability in n-type GaN epilayers. *Appl. Phys. Lett.* **96**, 242104 (2010).

### Acknowledgements

This work was supported by the National Natural Science Foundation of China (Nos 61306110, 61574004, 61361166007, and 61521004), the National Key Research and Development Program (Nos 2016YFB0400104, and 2016YFB0400201), the National High-Tech Research and Development Program of China (Nos 2014AA032606, and 2015AA016801), the National Basic Research Program of China (No. 2012CB619306), and Beijing Municipal Science and Technology Project (No. Z151100003315002).

### Author Contributions

Lei Guo and Xuelin Yang designed the experiments. Zhihong Feng, Yuanjie Lv, Jie Zhang, and Jianpeng Cheng performed the film growth. Lei Guo and Anqi Hu performed the characteristic measurement. Lei Guo and Xuelin Yang wrote the paper. Ning Tang, Xinqiang Wang, Weikun Ge, and Bo Shen gave scientific advices. Bo Shen supervised the project. All the authors contributed through scientific discussion.

### Additional Information

**Competing financial interests:** The authors declare no competing financial interests.

**How to cite this article:** Guo, L. *et al.* Hot electron induced non-saturation current behavior at high electric field in InAlN/GaN heterostructures with ultrathin barrier. *Sci. Rep.* **6**, 37415; doi: 10.1038/srep37415 (2016).

**Publisher's note:** Springer Nature remains neutral with regard to jurisdictional claims in published maps and institutional affiliations.



This work is licensed under a Creative Commons Attribution 4.0 International License. The images or other third party material in this article are included in the article's Creative Commons license, unless indicated otherwise in the credit line; if the material is not included under the Creative Commons license, users will need to obtain permission from the license holder to reproduce the material. To view a copy of this license, visit <http://creativecommons.org/licenses/by/4.0/>

© The Author(s) 2016